

1 Linköping studies in science and technology.
2 Dissertation, No. XXXX

3 ITERATIVE APPLICATION DESIGN IN SCIENTIFIC
4 VISUALIZATION

5

6 Alexander Bock



7

8 Division of Media and Information Technology
9 Department of Science and Technology
10 Linköping University, SE-601 74 Norrköping, Sweden
11 Norrköping, December 2016

The cover depicts...

12

Iterative Application Design in Scientific Visualization

13

14

Copyright © 2016 Alexander Bock (unless otherwise noted)

15

Division of Media and Information Technology

16

Department of Science and Technology

17

Campus Norrköping, Linköping University

18

SE-601 74 Norrköping, Sweden

19

ISBN: XXXX

ISSN: XXXX

20

Printed in Sweden by LiU-Tryck, Linköping, 2016

21

Acknowledgments

23 One of the best things about my experiences of the Swedish academic environment
 24 is its internationality. It will always remain strong in my mind.

25 My first and foremost thanks go to my two supervisors, Timo Ropinski and Anders
 26 Ynnerman, without none of this would have ever happened. Timo, who would have
 27 thought that me applying for a student technician job would ultimately lead to a
 28 Diploma thesis, a chance in country, and a PhD thesis in Norrköping. I will be ever
 29 grateful for the help and the opportunity; I have never looked back and regretted
 30 that 24 h decision to move northwards. Prof. Ynnerman, thank you for revitalizing
 31 my love everything space-related and providing me with the opportunity to work
 32 on these topics. Anders, tack för att du har introducerat mig för alla intressanta
 33 människor vid våra visningar tillsammans. Jag är skyldig dig en drink¹!

34 Thanks to all of my friends that I had the pleasure of meeting throughout the years.
 35 Indrē, ačiū už tai, kad manes neužmušei kai kažkas galéjo paminėti istoriškai netiklū
 36 šalies pavadinimą²; you, Johan, and Freja keep fabulous Norrköping safe! Paula,
 37 thanks for showing me around the world and being a good friend and moral com-
 38 pass; you do you! Saghi and Ehsan, بابت مهم ترین تعطیلات زندگیم از شما تشکر میکنم³.
 39 Daniel, for being my partner in crime; Umut, başından sonuna kadar (ve sonrasında
 40 da) iyi bir arkadaş olduğun için teşekkür ederim⁴; Erik, for making sure that every
 41 paper with you as coauthor got accepted; Martin, for proving that it is worth to
 42 go the extra mile; Stefan, for always being the perfect person to discuss intricacies
 43 of algorithmic details with; Khoa, my photography master; Rickard, the Lyapunov
 44 (pronunciation) expert; Sathish, shared pain is half the pain; Emil, I really wanted
 45 to put a Justin Bieber quote in here, but I couldn't find a fitting one; Joel, whose
 46 knowledge about stochastics still baffles me; Katerina, Carlo and Lucie, for too
 47 many good times to count; Andrew and Sherilyn, to Cologne!; Noeska, bedankt dat
 48 je contact met me hebt gehouden, ondanks dat ik gestopt ben met MedVis⁵; Big
 49 thanks also go, of course, to Joakim, Marcus, Åsa, Niclas, Jimmy, Andreas, Patric,
 50 Miro, Peter, and Jochen. Ευχαριστώ όλους τους Έλληνες φίλους μου που έκαναν
 51 την πόλη του Norrköping ενδιαφέρουσα: Ελένη (από το όμορφο νησί της Κύπρου),
 52 Μαρία, Νικόλαος, Αποστολία, Νίκος, Ελίνα και Βαγγέλης⁶.

53 همچنین از تمام دوستان ایرانیم علی، هدیه، نگار، آرش، فهیمه و مینا تشکر میکنم⁷

¹ Thanks for all of the interesting people that I met through our shows; I owe you a drink.

² for not killing me when someone might have mentioned a historically inaccurate country name

³ for taking me on the most important vacation of my life

⁴ for being a good friend from the beginning to end (and afterwards)

⁵ for not breaking off contact even after turning my back on MedVis

⁶ Thanks to all my Greek friends for making the city interesting: Eleni (close enough), Maria, Nikolaos, Apostolia, Nikos, Elina, and Vangelis

⁷ A big thanks to all my Iranian friends aswell: Ali, Hedieh, Negar, Arash, Fahimeh, and Mina.

A big thanks to all of the students that I had the pleasure of supervising over the years. You rock! Sandra, Martin, Victor, HC, Jonas, Michal, Anton, Karl-Johan, Tomas, Erik, Kalle, Michael, and Sebastian. 54
55
56

Thanks to Ingrid for helping out with many difficult questions and providing a new viewpoint on the value of applications. 57
58

To Eva Skärblom and Gun-Britt who helped out in so many different ways that would require their own dedication page. Thank you! 59
60

Big thanks to Carter who, in many ways, is the polar opposite of me. This only makes the combination unstoppable; to Masha, thank you for taking me in and for the trust throughout the years of collaboration; to Cláudio, for opening up the opportunity for a new exciting life phase. 61
62
63
64

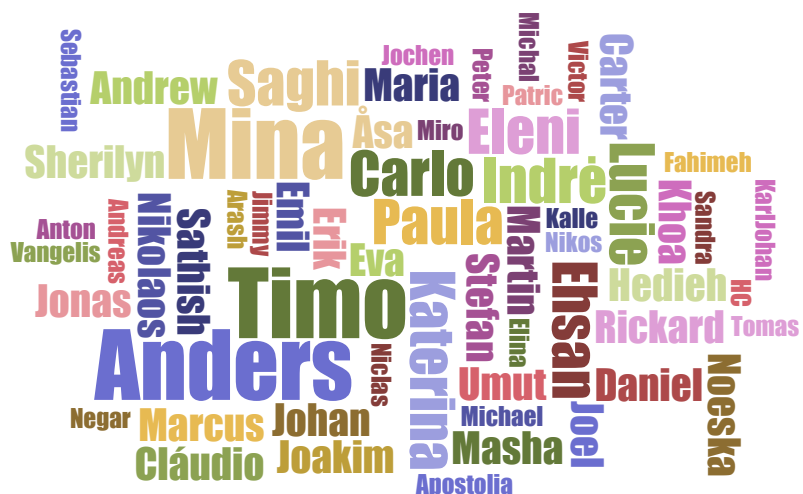
A collective thanks to everyone at the Visualization Center C in Norrköping. It is a privilege to work in a place to which other people travel for their vacations. 65
66

Question:
Which funding agencies and funding numbers should I put in here? 67

Vielen Dank an meine Familie für die lebenslange Unterstützung⁸! 68
To my incredibly understanding wife Mina. Meeting and marrying someone during the second half of a PhD must be the worst possible timing and, yet, she did not run away. I do not have more to say than عاشقٌ 69
70
71

Norrköping, November 2016

Alexander Bock 72



⁸ Thanks also to my family for the lifetime support

Abstract

74 Lorem ipsum dolor sit amet, consectetur adipiscing elit, sed do eiusmod tempor
75 incididunt ut labore et dolore magna aliqua. Ut enim ad minim veniam, quis
76 nostrud exercitation ullamco laboris nisi ut aliquip ex ea commodo consequat. Duis
77 aute irure dolor in reprehenderit in voluptate velit esse cillum dolore eu fugiat nulla
78 pariatur. Excepteur sint occaecat cupidatat non proident, sunt in culpa qui officia
79 deserunt mollit anim id est laborum.

Populärvetenskaplig Sammanfattning

82 Lorem ipsum dolor sit amet, consectetur adipiscing elit, sed do eiusmod tempor
83 incididunt ut labore et dolore magna aliqua. Ut enim ad minim veniam, quis
84 nostrud exercitation ullamco laboris nisi ut aliquip ex ea commodo consequat. Duis
85 aute irure dolor in reprehenderit in voluptate velit esse cillum dolore eu fugiat nulla
86 pariatur. Excepteur sint occaecat cupidatat non proident, sunt in culpa qui officia
87 deserunt mollit anim id est laborum.

Publications

- 89 The following list of publications have been included in this thesis:
- 90 **Paper A:** A. Bock, E. Sundén, B. Liu, B. Wuensche, and T. Ropinski. Coherency-Based Curve Compression for High-Order Finite Element Model Visualization. *IEEE TVCG (SciVis Proceedings)*, 18(12):2315–2324, 2012
- 93 **Paper B:** A. Bock, N. Lang, G. Evangelista, R. Lehrke, and T. Ropinski. Guiding Deep Brain Stimulation Interventions by Fusing Multimodal Uncertainty Regions. *Proceedings of the 2013 IEEE Pacific Visualization Symposium (PacificVis)*, pages 97–104, 2013
- 97 **Paper C:** A. Bock, A. Kleiner, J. Lundberg, and T. Ropinski. Supporting Urban Search & Rescue Mission Planning through Visualization-Based Analysis. In *Vision, Modeling, and Visualization*, 2014
- 100 **Paper D:** A. Bock, A. Kleiner, J. Lundberg, and T. Ropinski. An Interactive Visualization System for Urban Search & Rescue Mission Planning. In *International Symposium on Safety, Security, and Rescue Robotics*. IEEE, 2014
- 104 **Paper E:** A. Bock, Å. Svensson, A. Kleiner, J. Lundberg, and T. Ropinski. A visualization-based analysis system for urban search & rescue mission planning support. In *Computer Graphics Forum*. Wiley Online Library, 2016, in press
- 108 **Paper F:** A. Bock, A. Pembroke, M. L. Mays, L. Rastaetter, A. Ynnerman, and T. Ropinski. Visual Verification of Space Weather Ensemble Simulations. In *Proceedings of the IEEE Vis*, 2015
- 111 **Paper G:** M. E. Dieckmann, A. Bock, H. Ahmed, D. Doria, G. Sarri, A. Ynnerman, and M. Borghesi. Shocks in unmagnetized plasma with a shear flow: Stability and magnetic field generation. *Journal of Plasma Physics*, 2015
- 115 **Paper H:** Axelsson, Emil and Costa, Jonathas and Silva, Cláudio T. and Emmart, Carter and Bock, Alexander and Ynnerman, Anders. Dynamic Scene Graph: Enabling Scaling, Positioning, and Navigation in the Universe. In *Computer Graphics Forum, Proceedings of EuroVis*, 2017 (in submission)

- Paper I:** A. Bock, C. Emmart, M. Kuznetsova, and A. Ynnerman. OpenSpace: 119
Changing the narrative of public disseminations from *what* to *how*. In 120
Computer Graphics & Applications, 2017 (in submission) 121

- 122 The following publications, reported in reverse chronological order, are related to
123 the work described in this thesis, but have not been included:
- 124 • A. Bock, A. Pembroke, M. L. Mays, and A. Ynnerman. OpenSpace: An Open-
125 Source Framework for Data Visualization and Contextualization. Poster Presen-
126 tation at American Geophysical Union, Fall Meeting, 2015
 - 127 • A. Bock, M. Marcinkowski, J. Kilby, C. Emmart, and A. Ynnerman. OpenSpace:
128 Public Dissemination of Space Mission Profiles. Poster at IEEE Vis, 2015
 - 129 • A. Bock, M. L. Mays, L. Rastaetter, A. Ynnerman, and T. Ropinski. VCMass:
130 A Framework for Verification of Coronal Mass Ejection Ensemble Simulations.
131 Poster at IEEE VIS 2014, 2014
 - 132 • E. Sundén, A. Bock, D. Jönsson, A. Ynnerman, and T. Ropinski. Interaction
133 Techniques as a Communication Channel when Presenting 3D Visualizations.
134 In *IEEE VIS International Workshop on 3DVis*. IEEE Digital Library, 2014
 - 135 • S. Lindholm, M. Falk, E. Sundén, A. Bock, A. Ynnerman, and T. Ropinski.
136 Hybrid Data Visualization Based On Depth Complexity Histogram Analysis.
137 *Computer Graphics Forum*, 34(1):74–85, 2014, DOI: 10.1111/cgf.12460
 - 138 • S. Lindholm and A. Bock. Poor Man’s Rendering Of Segmented Data. In
139 T. Ropinski and J. Unger, editors, *Proceedings of SIGRAD 2013, Visual Compu-
140 ting, June 13-14, 2013, Norrköping, Sweden*, volume 094, pages 49–54. Linköping
141 University Electronic Press, 2013
 - 142 • K. T. Nguyen, A. Bock, A. Ynnerman, and T. Ropinski. Deriving and Visual-
143 izing Uncertainty in Kinetic PET Modeling. In *Proceedings of the EG Visual
144 Computing for Biology and Medicine*, pages 107–114, 2012
 - 145 • B. Liu, A. Bock, T. Ropinski, M. Nash, P. Nielsen, and B. Wuensche. GPU-
146 Accelerated Direct Volume Rendering of Finite Element Data Sets. In *Proceedings
147 of the 27th Conference on Image and Vision Computing New Zealand*, pages
148 109–114. ACM, 2012

Contributions

150 **Paper A:**

151 **Coherency-Based Curve Compression for High-Order Finite Element
152 Visualization**

153 Presents a novel rendering technique for real time visualization of non-linear finite
154 element models by introducing a preprocessing step in which potential rays are
155 computed by solving non-linear transformations and then compressed through the
156 use of B-splines. At rendering time during ray marching, these proxy rays are used
157 as an approximation as the transformations are not achievable in real time. The
158 method leads to a performance improvement of $15\times$ compared to a straight-forward
159 GPU implementation. This work was presented at IEEE VisWeek 2012.

160 **Paper B:**

161 **Guiding Deep Brain Stimulation Interventions by Fusing Multimodal
162 Uncertainty Regions**

163 In a participatory design with expert brain surgeons, this work presents a system
164 that supports Deep Brain Stimulation operations placing an electrode in the
165 patient's subthalamic nucleus. The presented system uses the available modalities,
166 such as preoperative CT/MRI scans, interoperative X-ray, probe measurements,
167 and patient responses, and fuses the available information into a multi-view system
168 that presents the available uncertainty ranges to the surgeon during the operation.
169 This work was presented at the IEEE Pacific Visualization Symposium 2013.

170 **Paper C:**

171 **Supporting Urban Search & Rescue Mission Planning through
172 Visualization-Based Analysis**

173 Presents a decision support system displaying a 3D visualization of point cloud
174 measurements obtained from partially collapsed buildings containing potentially
175 trapped and injured victims. The system uses these point clouds for a semi-
176 automatic path finding algorithm which suggests paths to an operator who uses
177 combined Scientific and Information Visualization techniques to analyse different
178 path attributes. This paper describes the results of an online study of this system
179 with nine international expert participants. This work was presented at the
180 International Symposium of Vision, Modeling, and Visualization in 2014.

Paper D:	181
An Interactive Visualization System for Urban Search & Rescue Planning	182
	183

This work presents an improved version of the decision support system published in Paper C focussed towards a presentation for rescue robots experts. More relevant aspects of an online user study are presented as well as implementations to be able to visualize the point cloud data, the paths, and derived data in immersive environments. This work was presented at the International Symposium on Safety, Security, and Rescue Robotics in 2014.

Paper E:	190
A Visualization-Based Analysis System for Urban Search & Rescue Mission Planning Support	191
	192

Based on the findings of Papers C and D, this work includes an adaptive sampling method that replaces the previous brute force sampling of the path search space for improved efficiency. Additional visualization techniques such as projective texturing and bump mapping are added to convey more information to the rescuer. Lastly, the work contains an additional eye-tracking user study with four rescuers. This work was published in Computer Graphics Forum in 2016.

Paper F:	199
Visual Verification of Space Weather Ensemble Simulations	200

Presents a visualization system developed in collaboration with space weather analysts for the use in the investigation of space weather phenomena. The system enables the comparison of in-situ measurements performed by satellites with time-varying volumetric simulations of the solar system. The system was designed in participatory design with the experts at the Community Coordinated Modeling Center, located at NASA's Goddard Space Flight Center and enabled new discoveries about the structure of in-flight coronal mass ejections. This work was presented at IEEE Vis in 2016.

Paper G:	209
Shocks in unmagnetized plasma with a shear flow: Stability and magnetic field generation	210
	211

In close collaboration with an expert in plasma simulations on submicroscopic scales, a system was developed to visualize the results of colliding ion beams. Under certain circumstances these collisions can form shocks, the dynamic structure of which was previously unknown prior to the initial visual inspection that was aided by the system. The work was published in the the Journal of Physics of Plasmas in 2015.

218 **Paper H:**

219 **Hybrid Data Visualization Based on Depth Complexity Histogram Anal-**
220 **ysis**

221 This work presents an algorithmic improvement on the A-Buffer implementation
222 that better utilizes cache locality on the GPU, thus improving the rendering
223 performance in mixed scenes containing both geometric and volumetric data.
224 These optimizations are founded on image-based analysis of the depth complexity
225 of different scenes and yield performance improvements of up to $8\times$ compared to
226 previous methods. This work was published in Computer Graphics Forum in 2014
227 and presented at SIGRAD 2016 and EuroVis 2016.

228 **Paper I:**

229 **Dynamic Scene Graph: Enabling Scaling, Positioning, and Navigation**
230 **in the Universe**

231 By utilizing a dynamic coordinate system origin, the framework described in this
232 work supports the simultaneous rendering of scenes with an extent that is larger
233 than the precision of floating points would otherwise allow. The paper analyses
234 the precision loss that occurs due to floating point arithmetic and, based on these
235 findings, presents a solution that operates on dynamically traversing a scene graph
236 structure. This work is in submission for EuroVis 2017.

237 **Paper J:**

238 **OpenSpace: Changing the Narrative of Public Disseminations from**
239 **What to How**

240 This work presents the open-source framework OpenSpace which supports the
241 interactive visualization of astronomical data in traditional and immersive envi-
242 ronments. The paper advocates the use of shared, immersive experiences as an
243 efficient medium of science dissemination to the general public and provides an
244 overview of the required techniques to achieve this. The examples presented in
245 the work include various space craft missions, such as New Horizons, Rosetta, and
246 Osiris Rex, as well as planetary rendering, and the space weather visualization
247 as described in Paper F. This work is in submission for Computer Graphics &
248 Applications 2017.

Contents 249

Acknowledgments	iii	250
Abstract	v	251
Populärvetenskaplig Sammanfattning	vi	252
List of publications	vii	253
Contributions	xii	254
1 Motivation	1	255
1.1 Applications	4	256
2 Introduction	5	257
3 Visualization Applications	7	258
3.1 Exploration Phase	9	259
3.2 Production Phase	9	260
3.3 Public Dissemination Phase	9	261
3.4 Evaluations	10	262
3.5 Comparison to Software Engineering	10	263
3.6 Domain areas	11	264
4 Iterative Application Design (contributions)	13	265
4.1 Overview	14	266
4.2 Biological and Medical Systems	14	267
4.2.1 Finite Element Visualization	14	268
4.2.2 Deep Brain Stimulation Interventions	21	269
4.3 Urban Search & Rescue	28	270
4.4 Astrophysics	28	271
4.4.1 Space Weather Visualization	28	272
4.4.2 Ion Beam Simulations	28	273
4.4.3 OpenSpace	28	274
5 Reflections	29	275
Bibliography	31	276
Paper A	41	277
Paper B	43	278

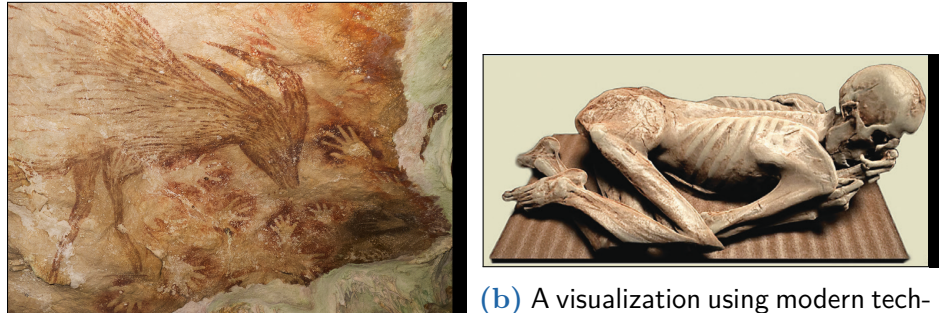
Contents

279	Paper C	45
280	Paper D	47
281	Paper E	49
282	Paper F	51
283	Paper G	53
284	Paper H	55
285	Paper I	57
286	Paper J	59

Motivation

289 Communicating intent and knowledge through visual means is maybe one of the
290 most distinct features that separate humans from other animals. Our ability to
291 intuitively understand abstract representations created by other humans from other
292 places or times has shaped the world's history immensely. The fundamental goal of
293 conveying information has not changed between the earliest cave paintings 40000
294 years ago (Figure 1.1(a)) and modern visualizations (Figure 1.1(b)). Humanities
295 focus on visual representations come from the fact that we are exceptionally good
296 at interpreting visual language by dedicating a large portion of our brain to this task.
297 While other senses might be more effective at accessing emotional information, the
298 visual cortex is the most effective way to ingest information. This is the reason
299 why we have spent so much effort and time on perfecting a visual language and
300 metaphors. As such, a good visualization is like a story; the author provides all
301 the necessary components, but the final assembly occurs in the beholder and is
302 thus subjective.

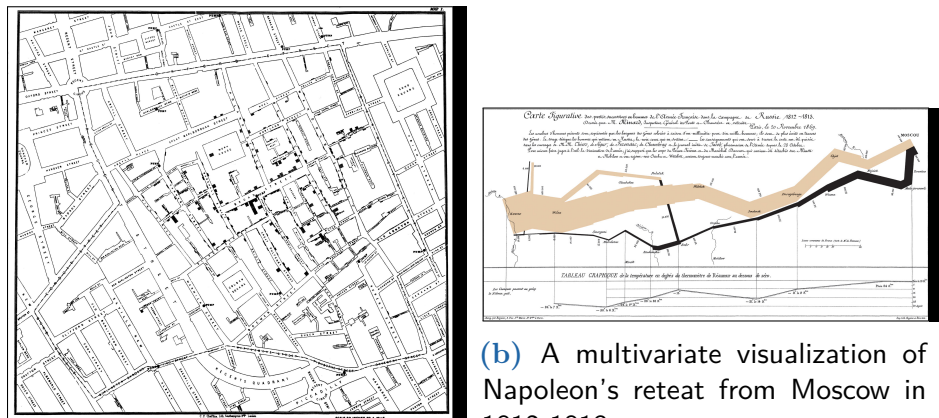
303 A good early example of the successful use of visualization is a spatial map of the
304 cholera outbreaks around Broad street in London in 1854 (Figure 1.2(a)). The
305 prevalent theory at the time for transmission of diseases was miasmatic and not
306 caused by germs. John Snow marked all cholera cases on a map and used this
307 visualization to pinpoint the origin of the outbreak — an infected pump [62]. While
308 this visualization seems simple by today's standards, it was an additional important
309 step towards establishing the germ theory of diseases. Another example was created
310 by Charles Joseph Minard in 1861 to visualize Napoleon's retreat from Moscow
311 in 1812 (Figure 1.2(b)). The map shows six different variables: geography, time,
312 temperature, the NapoleonâŽs movement, and the remaining number of troops.



(a) The earliest known human cave painting from around 38000 BCE. Image copyright by Maxime Aubert. Reprinted with permission.

(b) A visualization using modern techniques of a pre-dynastic Egyptian mummy. Image copyright by Daniel Jönsson. Re-printed with permission.

Figure 1.1: Two examples of human visualizations that are 40000 years apart. While the technologies changed drastically, the purpose of conveying information remains the same.



(a) A spatial visualization of cholera outbreaks around Broad Street in London in 1854.

(b) A multivariate visualization of Napoleon's retreat from Moscow in 1812-1813.

Figure 1.2: Two well-known examples of visualization used to produce scientific insight (Figure 1.2(a)) and inform the general public about complicated data (Figure 1.2(b))

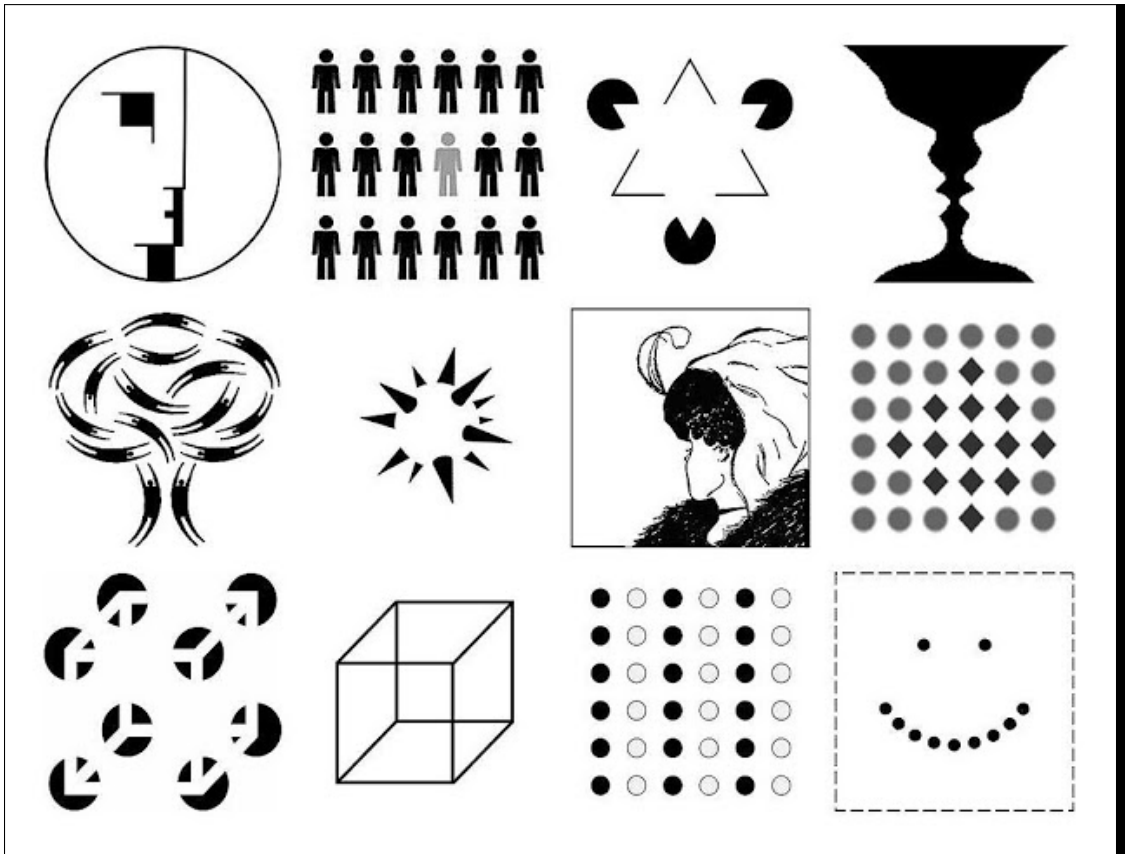


Figure 1.3: Examples of Gestalt theory ... Change image

313 The layout and design and its ability to show Napoleon’s terrible fate in Russia has
 314 caused this graphic to be called “the best statistical graphic ever drawn” [70]. In
 315 his books, Tufte provides many more good examples of visualization mixing design
 316 and information representation [69]. All of these examples show an important
 317 difference in purpose between visualization and computer graphics, which is also
 318 exemplified in Ben Shneiderman’s quote that “the purpose of visualization is insight,
 319 not pictures”. Instead of generating images devoid of information, the purpose of
 320 visualization is to create images that enable a person to derive insight.

321 These examples also make subconscious use of one of the remarkable aspects of
 322 human perception. We are capable of analyzing scenes both preattentive as well as
 323 attentive. Preattentive perception happens when features of an image *pop out*, or
 324 are obvious to the beholder without conscious effort. Figure 1.3 shows an example
 325 of this effect using the Gestalt theory [75]. In his work, Wertheimer found that
 326 attributes like closure, similarity, or continuation enable an observer to perceive
 327 a collection of objects as a continuous form (or *Gestalt*). This characterization is
 328 performed preattentively and largely independent of the number of objects that
 329 are involved. He also investigated what objects can be added to these groupings

before the continuous form is destroyed.

330

1.1 Applications

331

As alluded to in the two examples provided above, visualization cannot occur 332
realistically when a specific *target domain* or *problem domain* is considered. Except 333
basic research, all visualization research has to take the domain into account and is 334
meaningless on its own. Even for basic research, its effectiveness is important and 335
has to be proven. The different domains are frequently tackled with visualization 336
applications that are tailored to a *domain expert*, who is interested in understanding 337
a specific aspect of their data. The design of a visualization application requires 338
knowledge from many different fields, such as computer science, perception, cogni- 339
tion, interaction design, or art, and is thus in itself multidisciplinary [47]. The design 340
process furthermore requires in-depth knowledge about the domain and therefore 341
demands interdisciplinary collaborations with experts from other fields [31]. 342

Over the past years, the field of visualization has matured to the degree that basic 343
research on novel visualizatoin techniques is being replaced with application-driven 344
research that applies the generic toolset the community has acquired. Even though 345
most problems require a custom solution to some extent, it is still possible for the 346
visualization community as a whole to benefit from the reasearch on individual 347
applications as they feed back into the general knowledge base. This feedback loop, 348
combined with the insight that custom solutions are required for the majority of 349
non-trivial tasks, excluded the use of ready-made programs as well. 350

351

352

Introduction

- 353 • SciVis / InfoVis / VAST
 - 354 – it's all the same, but different flavors) [not too long]
 - 355 – (solving the same problem with different tools)
 - 356 – [17] [66]
 - 357 – The Value of Visualization v.Wijk [71]
 - 358 * Referencing "The Death of visualization" paper
 - 359 – Dangers of visualization [43]
 - 360 * Showing incorrect information
 - 361 * Showing information incorrectly
 - 362 * Cultural component in understanding visualizations
 - 363 • Visualization pipeline
 - 364 – OpenGL Graphics pipeline [60]
 - 365 – Image of visualization pipeline (haber and mcnabb)
 - 366 – Multiple locations for modifying the results [Mulder et al., 1999]
 - 367 – Data acquisition
 - 368 * Data types
 - 369 * Modalities (CT, MRI, simulations)
 - 370 * Different grids (cartesian v spherical)

6 Chapter 2 • Introduction

– Direct Volume Rendering	371
* Emission/absorption [59]	372
* Volume rendering integral [46]	373
* Other techniques	374
· MIP / MIDA / isosurface	375
· Object-order: texture slicing [76], splatting [77]	376
· Image-order: volume raycasting [22, 35, 59] speedup: [33] single pass rendering [28, 64]	377
* Raycasting v raytracing	378
– Explaining multiviews, brushing, linking, etc (Tory 2003)	380
– More information in Real-Time Volume Graphics: [23]	381
• Combination of automated systems and human-in-the-loop; Shows importance of domain expert integration	382
– Interaction design	383
– [51] [71] -> Shows importance of domain expert integration	384
	385

Visualization Applications

388 Point of the chapter

- 389 • "introduces the concepts that i have used in my work"
- 390 • Telling a story that leads up to contribution
- 391 • Shortest path for a new person to understand the contributions
- 392 • "This is what people think about collaboration and I did that"
- 393 • "Supported claims, needs more academic tone"
- 394 • "Generic, explain the methodolgry"
- 395 • Different kinds of application requirements [Tamara Munzner's papers]. Different stages
 - 396 – Exploratory for single dataset (information gathering)
 - 397 – Repeating the same processes for multiple datasets (doctors in hospital)
 - 398 – Public dissemination of data
- 400 • Evaluations
 - 401 – Many papers in InfoVis on evaluation
- 402 • Usefulness of convincing a domain expert of the usefulness of a visualization technique
 - 403 – Obviously, there are visualization techniques that are not intuitively understandable, but useful nonetheless

8 Chapter 3 • Visualization Applications

- For example: Parallel coordinates plot [USAR evaluation] 406

Collaboration workflow

407

The usual workflow of both types of collaborations is the following: 1. Initial contact: Depending on the category of collaboration this is initiated by either the domain expert or the visualization researcher and consists of a cursory introduction into each others fields. The domain scientist provides a limited introduction into the they research topic and the visualization expert brainstorms various techniques that might prove beneficial. 2. Data retrieval: The first step to every collaboration is the development of interfacing techniques. Usually, visualization researchers have access to a growing toolkit of visualization techniques int which the domain experts data has to be imported. In some cases, this might be trivial (for example, loading RAW data), whereas other cases might prove more difficult (for example, converting between grids) 3. Feasibility study: Usually at this step, the visualization researcher has to assess whether there is any potential research in the collaboration. This step is probably one of the most challenging ones as the goals of the different parties might diverge. A novel visualization technique that might be beneficial to the visualization researcher might not be accepted by the domain scientist, complicating the collaboration. This step is furthermore complicated by the fact that some projects do not have an initial payoff in novel visualization techniques, but have the promise of future benefits once an initial collaboration is established. 4. Application design: In this step, the visualization researcher and the domain expert collaborate in varying degrees on designing the application. On the visualization side, this consists of attaining a cursory knowledge of the subject matter as well as developing the application itself. On the domain expert side it consists of providing knowledge about his field, experimenting with the software, and providing feedback. 5. Publish results: The results of the collaboration are published in both the visualization field as well as the scientific domain of the expert.

432

Old

433

- Different phases for applications 434
- Different kinds of application requirements 435
- Some applications might move between phases 436
- Some are never designed to move 437
- Interplay between Visualization and applications from a scientific (= domain expert) point of view 438
439
- Important aspect for applications: What are the generalizable aspects that other people can use 440
441

- 442 • [50] Main paper; four layer model; validation and iterative loops
- 443 • [67] Different approaches for system construction (design philosophies)
- 444 • [31] Sci collaborations across disciplines; interdis, multidis, intradis; definition
- 445 of a domain expert
- 446 • [72] kinds of gaps; knowledge gap and interest gap; different cooperation models
- 447 • [74] Guidelines for multiview setups in information visualization
- 448 • Combining multiple applications to deal with a problem [58]
- 449 • "Participatory design"
- 450 • Different kinds of application requirements: exploration, production, dissemina-
- 451 tion
- 452 • Learning about the terminology that experts use

453 3.1 Exploration Phase

- 454 • Exploratory for single dataset (information gathering)
- 455 • Initial information gathering
- 456 • Hypothesis forming (first visualization of a new phenomenon)

457 3.2 Production Phase

- 458 • Repeated information gathering (generating tools for looking at the same kind
- 459 of data over and over)
- 460 • Applying the same techniques to more datasets
- 461 • Repeating processes on multiple datasets

462 3.3 Public Dissemination Phase

- 463 • Presenting information to the general public
- 464 • Public dissemination
- 465 • Robustness
- 466 • "Publish and perish": Case that even though papers are published, having a
- 467 public outreach might reach many more people
- 468 • Targeting not domain scientists, but the public audience at large

10 Chapter 3 • Visualization Applications

- 3D Interaction gestures 469
- "In software engineering, validation is about whether one has built the right product, and verification is about whether one has built the product right." 470
(Munzner, Nested Model) 471
472

3.4 Evaluations

473

- – Many papers in InfoVis have been written about evaluations 474
 - How are they applicable to scivis or vis in general 475
- [68] How to perform expert usability studies 476
- [32] Different reasons for user studies; alternatives to user studies; hard to 477
publish null results 478
- [18] InfoVis evaluation; system v system has bias towards familiar system; 479
applicable to scivis? eval has mixture factors; type 1 v type 2 errors; participatory 480
observation (collaborative work with experts) 481
- [36] Think aloud protocol introduction to the HCI community 482
- [24] Variation on the think aloud protocol to only mention actions rather than 483
thoughts 484
- [37] Introduction of the Likert scale 485
- [53] Usability heuristics 486
- Evaluations [54] (how to report evaluations: [26]) 487
- User studies 488
 - Domain expert needs to be involved in finding the people that want to 489
participate in a study 490
 - How do you deal with the requirement of a user study in very limited field? 491
[Space Weather] 492

3.5 Comparison to Software Engineering

493

- Tamara Munzner's nested design is similar to software engineering waterfall 494
([57, 73]) model (make a bigger point out of this?) 495
- Make comparisons to Scrum + sprints 496

497 **3.6 Domain areas**

- 498 • Moving all of the background information from Chapter 4 into this
499 • Define challenges that are picked up by the contributions

500

501

502

Iterative Application Design (contributions)

- 503 • Exploratory for single dataset (information gathering)
 - 504 – Paper 1 (FEM)
 - 505 – Paper 7 (Shocks)
- 506 • Repeating the same processes for multiple datasets (doctors in hospital)
 - 507 – Paper 2 (DBS)
 - 508 – Paper 3, 4, 5 (USAR)
 - 509 – Paper 6 Space Weather
- 510 • Public dissemination of data
 - 511 – Paper 8 (OpenSpace)
 - 512 – Paper 9 (DSG)

513 Old

514 This chapter describes the contributions of all papers that are included in the thesis
515 and them to the descriptions about application design as described in the previous
516 chapter. The following sections first describe the separation of papers into topic
517 areas and then elaborate on each of the topics.

4.1 Overview

518

Due to the varied nature of application papers, this papers are separated into three 519
topic areas: 520

Biological and Medical Visualization. Paper A and Paper B deal with 521
algorithmic and application design challenges regarding biological simulation and 522
medical intervention support respectively. Paper A describes an algorithm that was 523
developed to effieciently render non-linear finite element models; Paper B describes 524
an application system used in deep brain stimulation interventions. (Section 4.2) 525

Urban Search & Rescue. Paper C, Paper D, and Paper E describe the 526
collaborative work on designing a visualization system to support urban search & 527
rescue operators and rescuers. The system utilizes 3D point cloud data as the basis 528
for a pathfinding algorithm, whose results are presented to the expert user for a 529
human-in-the-loop decision support. (Section 4.3) 530

Astrophysical Phenomena. The papers in this topic deal with visualization 531
system that were performed to deal with astronomical and astrophysical phenomena. 532
Paper F and Paper H describe visualization systems that are applied to space 533
weather and ion simulations respectively, where as Paper G describes the required 534
algorithm necessary to achieve these systems. (Section 4.4) 535

Each of the topics provides a short introduction into the domain and, then, elaborate 536
on the work that has been done in the respective papers. 537

4.2 Biological and Medical Systems

538

- Describe background and previous work in biological visualization + systems 539
- Describe background and previous work in medical visualization + systems 540
- Medical visualization as one of the first expert domains 541
- Support for the operating theater 542
- General problems with medical visualization 543
 - Hard to convince people to use it: 544
 - Certification / limited time of the physicians 545
- More information about medical visualization [55] 546

4.2.1 Finite Element Visualization

547

In this project we developed an algorithm for real-time volume rendering of multi- 548
variate non-linear finite element model (FEM) simulations. One of the datasets 549
that was in the focus was a simulation of a human heart that calculates the stress 550

551 tensor at each location during a cardiac cycle. By comparing the results of healthy
 552 and abnormal hearts, it becomes possible to detect structural defects before they
 553 manifest [79, 80]. Traditionally, these models are visualized using iso-surfaces or
 554 glyphs [78], but not using volume rendering. As was stated in Section ??, the
 555 value for each sampling point during the volume ray marching has to be fetched
 556 for a correct front-to-back compositing. This step becomes a bottleneck in the
 557 case of non-linear FEM datasets, as the data access becomes non-trivial, thus
 558 reducing rendering speeds to non-interactive levels. Paper A describes an algorithm
 559 that utilizes a precomputation step to cache a reduced set of possible rays that
 560 are then used in the rendering to efficiently access the data, resulting in a 15×
 561 performance gain, relative to straight-forward GPU implementations, which in turn,
 562 is an improvement of 2 to 4 orders of magnitude compared to a straight-forward
 563 CPU implementation [41].

564 Background

565 FEM methods are used extensively in a large number of fields, for example en-
 566 gineering, construction, or biology, as an approach to solve complex problems
 567 numerically. For these methods, the problem domain is separated into a finite
 568 number of cells over which the numerical simulation can be performed efficiently.
 569 For more information, we refer the reader to the book by Bathe and Wilson [3].
 570 For our purposes it suffices to know that each element is associated with two
 571 coordinate systems. The location and deformation of each element is specified in
 572 *world coordinates*, whereas the computed values are stored in a material coordinate
 573 system ξ which, in most cases, is of a simple geometry such as cubes, triangles, or
 574 tetrahedra. For each FEM, there exist a bilinear transformation between the nodal
 575 points expressed in either coordinate system. The variates of study are defined in
 576 the material coordinate space and are interpolated using trilinear interpolation.
 577 The transformation between world coordinates and material coordinates can be
 578 arbitrarily complex and undoing these transformations is at the heart of the mis-
 579 sion performance to be able to render these models interactively using volumetric
 580 rendering techniques.

581 When performing volume raycasting on the FEM, the individual rays for each
 582 pixel are defined in world coordinates and are straight lines. For each element
 583 that is intersected by a ray, each rays have to be converted into the material space
 584 for the value lookup. This transformation turns a straight ray into a curved ray
 585 (see Figure 4.1(c)) which necessitates coordinate transformations during the ray
 586 marching. Due to the nonlinearity of these transformations, multidimensional iter-
 587 ative approaches such as the Newton method have to be used, further exasperating
 588 the performance loss.

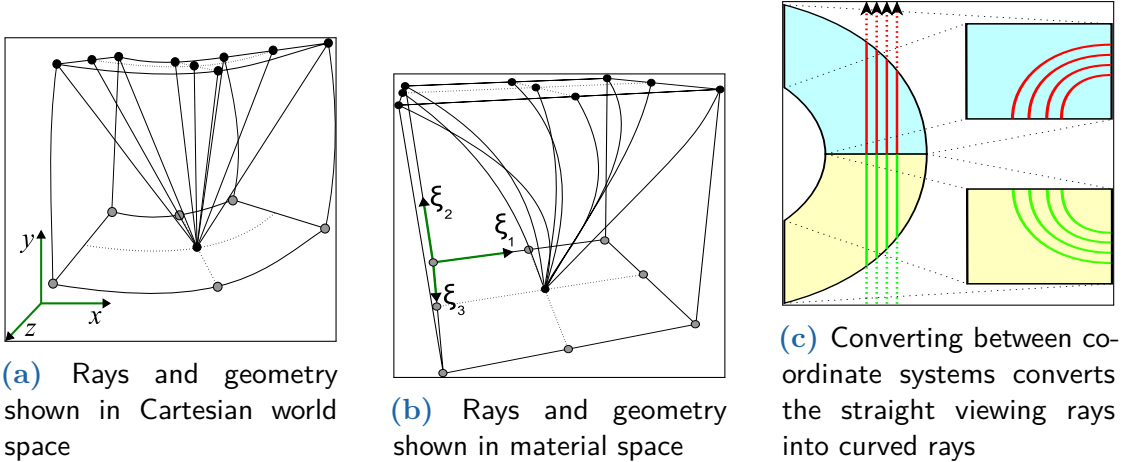


Figure 4.1: These images demonstrate the transformation between world coordinates and material coordinates for a set of viewing rays when viewing the element geometry and the viewing rays from the world (a) or the material (b) coordinate system.

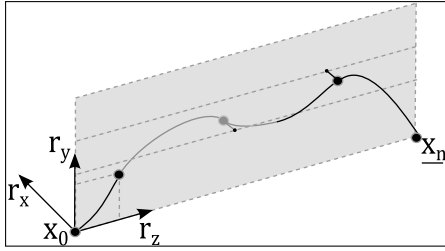
Algorithm

589

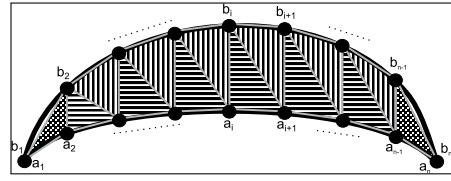
As the previous session demonstrated, it is detrimental to the interactive performance to convert from material space to world space at rendering time. Therefore, we utilize a precomputation step in which many of the possible ray combinations through the different elements are solved and stored as *proxy rays*. At rendering time, we then need to collect the correct ray and can then use that information to fetch the data values at their correct locations. Computing all possible proxy rays would require an infinite amount of memory, so we make some approximations that lead to data reduction. 590
591
592
593
594
595
596
597

Proxy ray generation First, we do not store the entirety of a proxy ray, but sample it in a few points and use these as control points for a Catmull-Rom spline [19] from which we can reconstruct the original path. The number of control points that are used to approximate each ray is a user-defined parameters. The optimal parameter for this value depends on the complexity of the dataset (see Section 4.2.1). 598
599
600
601
602
603

Second, we compute only a finite number of proxy rays for each element by creating a uniform grid on each of the elements surface and computing all proxy rays between pairwise combinations of grid points. Figures 4.1(a) and 4.1(b) show a potential set of these rays for an element in world coordinates and material space. We can apply this approximation since well-behaved finite element simulations usually do not produce degenerate elements for which a much higher resolution is needed. 604
605
606
607
608
609



(a) Increasing the similarity between splines by converting them into a common coordinate system.



(b) A representation of the metric that is used in the K-Means clustering algorithm, approximating the area between the two rays by a sum of the triangle areas.

610 **Clustering** Even with these approximations, the amount of spline data for the
 611 entire FEM dataset is still unmanageable for the GPU. Since there is a potential for
 612 a high degree of similarity between rays even across elements due to symmetries
 613 and bounded ray complexity, we can utilize a clustering algorithm to reduce the
 614 number of representative proxy rays necessary for the rendering.

615 The first step for the clustering is to increase the similarity between proxy rays
 616 while maintaining the ability to uniquely reconstruct the final ray. For this, all
 617 rays are converted into a common coordinate system in which the first P_1 and the
 618 last P_n control point are located on the z axis. Then, all control points are rotated
 619 around the z axis such that the first point P_i that is not collinear with P_1 and
 620 P_n is in the yz plane. This rotation angle θ is retained. Lastly, all control points
 621 are scaled along the z axis such that P_n becomes equal to $(0, 0, 1)$. Figure 4.2(a)
 622 shows the results of these transformations on an example ray. Both the translation
 623 and the scaling can then later be undone during the rendering without storing
 624 additional information, as the entry and exit points (and their distance) are known.

For the clustering of the splines, we make use of the variant of the K-Means [30] algorithm due to its stability and ability to deal with values of arbitrary dimensions. For this, we adapt an idea from Abraham et al. [1] and perform the clustering on the control points of the Catmull-Rom splines directly. The metric for the clustering uses the area between two curves as approximated by a Riemann sum of triangles connecting the proxy rays, sampled at a high frequency (see Figure 4.2(b)). For two proxy rays a and b , and their n sampled points a_1, \dots, a_n and b_0, \dots, b_n with $a_1 = b_1$, $a_n = b_n$, $\exists i \in [2, n - 1] : a_{i_x} = 0$, and $\exists j \in [2, n - 1] : b_{j_x} = 0$ due to the transformation performed in the last paragraph, the similarity metric is defined by:

$$\begin{aligned} d(a, b) = & \frac{1}{2} \left(\|a_1 a_2 \times a_2 b_2\| + \right. \\ & \sum_{i=2}^{n-2} \|a_i a_{i+1} \times a_i b_i\| + \|b_i b_{i+1} \times b_{i+1} a_{i+1}\| + \\ & \left. \|a_{n-1} a_n \times a_{n-1} b_{n-1}\| \right) \end{aligned} \quad (4.1)$$

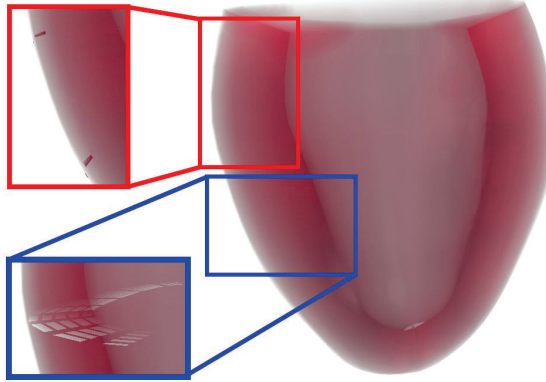
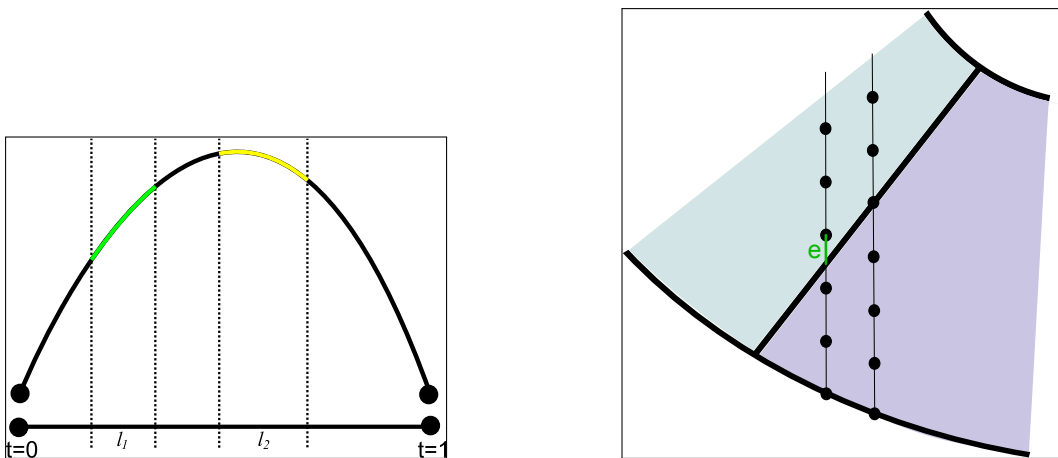


Figure 4.3: The insets show potential rendering artifacts when applying the depth peeling algorithm to finite element methods.

After applying the clustering, for each original point we now have a cluster identifier 625
for the representative ray and the angle θ as computed above. 626

Rendering During the rendering step of the algorithm, the proxy geometries for 627
all elements are rendered. The material space coordinates are mapped to the RGB 628
channel, as described by Krüger and Westermann [33], and the face identifier and 629
element identifier are encoded in the transparency channel. We then render the 630
entire scene in multiple passes, employing a modified depth peeling approach as 631
described by Everitt [25] for each of the passes. A usual problem problem with 632
depth peeling is z-fighting, where the depth of multiple geometries are too close in 633
screenspace to be discriminated. This is especially true for finite element models 634
where the elements by construction have to touch each other. In order to remove 635
the artifacts that would otherwise occur (see Figure 4.3), we use the fact that 636
faces of different elements have the same world coordinates and we can filter those 637
elements by their respective normals as we know that the two faces of the touching 638
elements must of opposite normals. 639

For each of the peeling rendering steps, we can then use the color information 640
for each pair of fragments to retrieve the entry and exit points as well as the 641
face and element ID. Using this information, we can retrieve the cluster ID and 642
the angle θ of the proxy ray that belongs to the fragment pair. The previous 643
transformations of the proxy ray can be undone in the following way: First, the 644
proxy ray is scaled by the distance between the entry and exit points in world 645
coordinates. Second, it is translated and rotated such that P_1 coincides with the 646
entry point and P_n coincides with the exit point. Then, the proxy ray is rotated 647
by θ around the axis connecting P_0 and P_n . The ray marching can then interpolate 648
along the Catmull-Rom spline to retrieve the correct sampling value in material 649
space. This ray marching cannot, however, take place in the material space as this 650
would lead to a non-uniform sampling in world space (see Figure 4.4(a)). Therefore, 651



(a) The desire to uniformly sample the view ray in world space requires an arclength parametrization of the proxy ray.

(b) Special border handling is required between elements, as a naïve implementation would oversample the boundary.

Figure 4.4: Utilizing the proxy rays for ray marching in material space introduces two potential sources of non-uniform sampling in world space.

the spline interpolation parameter $t \in [0, 1]$ has to be converted into an arclength parametrization such that the sampling in material space becomes non-uniform to make the world space sampling uniform instead [27]. A second subtle error occurs at the boundary between elements and is exemplified in Figure 4.4(b). Restarting the ray marching at each element would also lead to a non-uniform sampling and thus rendering artifacts. For this reason, the remaining distance between the last sample and the exit point is stored at the end of the ray marching and this distance is used to offset the first sampling point in the following element, similar to the method employed by Ljung [42].

Lastly, we employ another technique to mitigate rendering artifacts that stem from a low sampling resolution of proxy rays. If, for example, each face uses only a 3×3 grid of points, the same proxy ray will be used for a large area of the face; similar to nearest neighbor interpolation. To remedy these artifacts, we effectively use bilinear interpolation on the control points of the four closest proxy rays and perform the ray marching along the spline generated by these interpolated control points. This interpolation method is called *intra-ray interpolation*. A second interpolation method is called *intra-ray interpolation*, where all rays with entry and exit points exchanged are fetched. These are then sampled with $t' = 1 - t$ and the two results are averaged before sampling the volume. Figure 4.5 shows the difference on the heart dataset, where 5×5 rays per face for each element were generated.

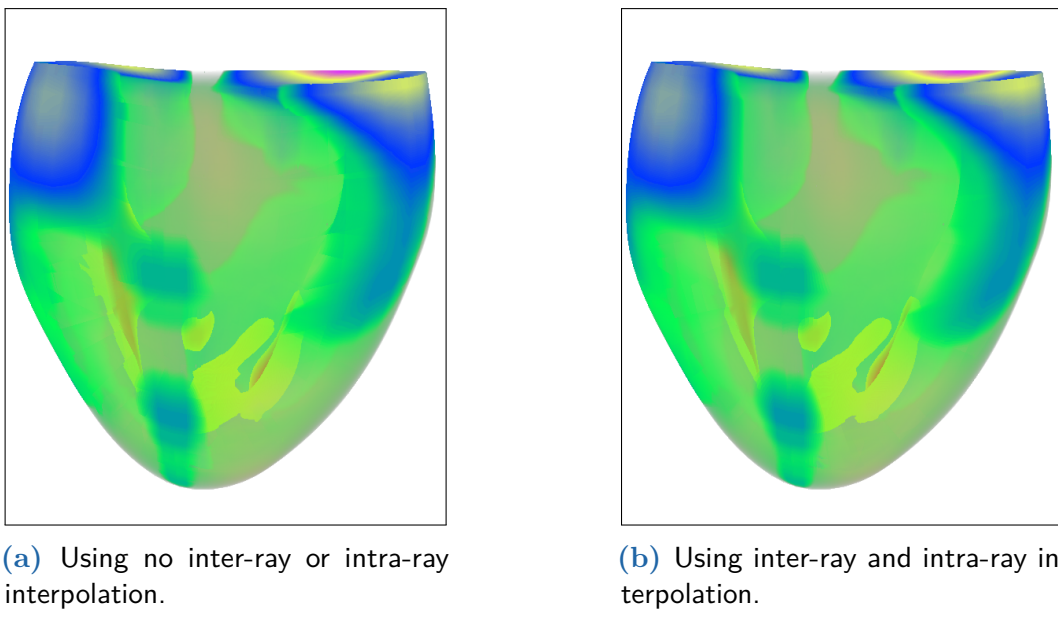


Figure 4.5: A volume rendering of the heart dataset using 5×5 rays per face for each element showing the difference between the interpolation schemes.

Results	673
Generalization	674
• Rendering multi-variate non-linear finite element models	675
• Transformation from linear rays in world-space to curve rays in material space	676
• Simulation values are described in material space	677
• Transformation from world to material space is computationally expensive (multi-dimensional Newton method requires multiple iterations involving the Jacobian)	678 679 680
• Solve by using precomputation step to compute proxy rays for each element	681
• Precomputation is allowable as the elements are usually not degenerate and smooth	682 683
• During rendering time, proxy rays are used to look up values in the finite elements and perform the ray marching	684 685
• Proxy ray computation	686
• Voreen: [48]	687
– Create a uniform grid on the surfaces of each element	688
– Compute rays from each grid cell to each other grid cell	689

- 690 – Collect all proxy rays and store a limited number of control points used for
691 Catmull-Rom spline interpolation
- 692 – Move them into a common coordinate system (one point into origo, linear
693 scaling, rotating all splines such that P0, Pp, Pn lie in the yz plane [P0 and
694 Pn already on z axis from normalization], Pp is the first non-collinear point).
695 Store θ from the rotation
- 696 – Perform clustering on the proxy rays [1] with K-means [30]
- 697 – Metric for clustering is the area covered between two splines
- 698 – Allow for potential different grid resolutions on entry v exit faces -> importance-
699 based ray sampling
- 700 • Rendering
 - 701 – Depth peeling
 - 702 – Lookup ray id and θ
 - 703 – Bend and rotate closest ray into place
 - 704 – Perform ray marching along the proxy ray (arc parametrization to take into
705 account the different lenghts in material and world space [27])
 - 706 – Intersegment handling of sampling points (we do not want to start the sampling
707 at the beginning, but have a continuous transition between elements)
 - 708 – Inter vs intra ray interpolation
 - 709 * Inter: bilinear lookup between four closest ray matches and perform inter-
710 polation between spline results
 - 711 * Intra: Retrieving the opposite ray (entry->exit; exit->entry) and looking
712 up at t and $1 - t$ and interpolate between

713 4.2.2 Deep Brain Stimulation Interventions

714 In we work package of Paper B, the task was to develop a medical visualization
715 application for deep brain stimulation (DBS) intervention support in collaboration
716 with physicians at the St. Barbara Hospital in Hamm, Germany. This system should
717 be designed to support the brain surgeon during the surgery in order to achieve a
718 higher precision and thus a higher probability of a positive outcome for the patient.
719 In contrast to other medical domains, where the doctor's available preparation time
720 for each patient is limited and thus procludes any complex interaction techniques
721 on visualization applications, DBS interventions already have a long planning phase
722 scheduled prior to the operation, thus enabling the usage of specialized tools and
723 providing the ability for visualization to play an important role in this scenario.

Question: Is this too much a retelling of the paper story? If so, what additional information should be in here?

The application resulting from this collaboration combines an enhanced multimodal 724
 3D volumetric rendering environment with the spatial visualization of electric 725
 measurements that are recording the patient's brain activity during the proce- 726
 dure in combination with patient-specific ability tests. Spatially embedding the 727
 measurements with the volumetric information reduces the cognitive load of the 728
 surgeon during the procedure, as this mental link does not have to be performed 729
 by the surgeon themselves. Furthermore, the system shows the uncertainties of the 730
 different modalities in a single view, thus enabling the surgeon a comprehensive 731
 view and more insight during the procedure. 732

Background

733

With the system, we target DBS interventions that are performed on patients' 734
 afflicted with Parkinson's Disease or other forms of essential tremors. During 735
 these interventions, a stimulating electrode is inserted into patients' brains that 736
 has the potential to inhibit some of the debilitating effects of these tremors [29]. 737
 A potential beneficial target region for the electrode location is the patient's 738
 subthalamic nucleus (STN) [4]. However, the STN is a relatively small structure 739
 with the size of a few millimeters [56] and a location deep inside the patient's brain. 740
 Furthermore, it is not detectable in MRI scans in some patients [63] and thus hard 741
 to localize. The intervention is further complicated as a small deviation in the 742
 electrode's location will excite other parts of the patient's brain that can lead to 743
 undesired memory or speech impairments. 744

In addition to traditional imaging modalities, the system makes use of Micro- 745
 electrode Recordings (MER) [34] capable of recording the electrical activities in 746
 different parts of the brain. The MER system consists of a small group of electrodes 747
 that measure the brain's electric field around them. The relative amplitude and 748
 frequency of these fields correlate with the specific brain region that the electrode 749
 is in [5] and can thus be used to determine whether the electrodes are in the 750
 correct locations inside the patient's brain. The results of the MER recordings are 751
 traditionally reviewed on loudspeakers that are placed in the operating room. Aside 752
 from the obvious drawbacks of a limited auditory channel, potential background 753
 noise, and limited echoic memory, a big issue is the surgeon's mental separation 754
 between the spatial location of the electrodes and their measurements. This holds 755
 true for both the absolute location of the electrode cluster inside the brain, as well 756
 as the relative positions of the electrodes inside the cluster. 757

Problems that were not sufficiently solved by previous methods include the fusion 758
 of the available modalities. These modalities include pre-operative CT and MRI 759
 scans, interoperative X-Ray scans, the electrode measurements during the insertion, 760
 and patient tests after the final electrode has been activated. Making efficient 761
 use of all available information is important as the principal limiting factor for 762
 the maximum operation length is the patient's ability to cooperate, as a DBS 763

764 intervention is very taxing to the patient as they have to be awake during the entire
 765 procedure which can last up to 10 hours.

766 A DBS procedure is split into three distinct phases. In the first phase, the *planning*
 767 phase, the surgeon plans the operation by locating and segmenting the most
 768 probable location of the STN using preoperative CT and MRI scans. Using other
 769 tools [61], an optimal access channel is then planned that evades important sensitive
 770 brain regions and selects the optimal location for the electrode to affect the STN [16].
 771 In the second phase, the *recording* phase, the patient is in the operating room with
 772 their head in a stereotaxic frame, that restricts the movement and thus allows for
 773 a fixed-body transformation between the patient and the operating room, used
 774 for later registration. The MER sensors are inserted into the patient's brain along
 775 the preplanned access path until they have reached the planned depth. During
 776 this phase, the measurements of the electrodes are used to distinguish the different
 777 adjacent brain regions. If the electrodes correctly identify the STN region, the
 778 depth along the access path is noted and the electrodes' location is verified with
 779 bi-planar X-ray scans. After this verification, the electrodes are retracted. In the
 780 third phase, the *placement* phase, a transmitting electrode is inserted into the access
 781 path to the same location that was measured during the previous phase. Once the
 782 electrode is in place, it is activated and its output is tuned. Using interoperative
 783 bi-planar X-ray scans and markers on the stereotactic frame, the location of the
 784 electrode inside the patient's brain is verified. Then, utilizing patient tests that
 785 examine the patients' ability, such as long term memory ability and measuring
 786 the tremor, the location of the electrode might be adjusted until an acceptable
 787 response is achieved or the patient is no longer capable of cooperating due to the
 788 length of the procedure.

789 System

790

791 In close collaboration with the surgeons, we created a system that can ingest
 792 the access path planned using other sophisticated tools (see Figure 4.6), the
 793 various scans (T_1 and T_2 MRI, CT, and X-Ray), the MER measurements, as
 794 well as the patient tests during the operation. Combining all available modalities
 795 into one system enables the surgeon to inspect all available information for both
 796 operational phases. The system consists of multiple linked views. The *Contextual*
 797 *view* is available in both phases, whereas the *2D audio visualization* and *3D audio*
 798 *visualization* are only available in the recording phase and the *Target closeup* and
 799 *Placement guide* are only available in the placement phase. The rest of this section
 800 elaborates on the design decisions for the individual views.

Question:
Should I use
“I” or “we” in
the text?

801

Question:
How detailed
should this
be?

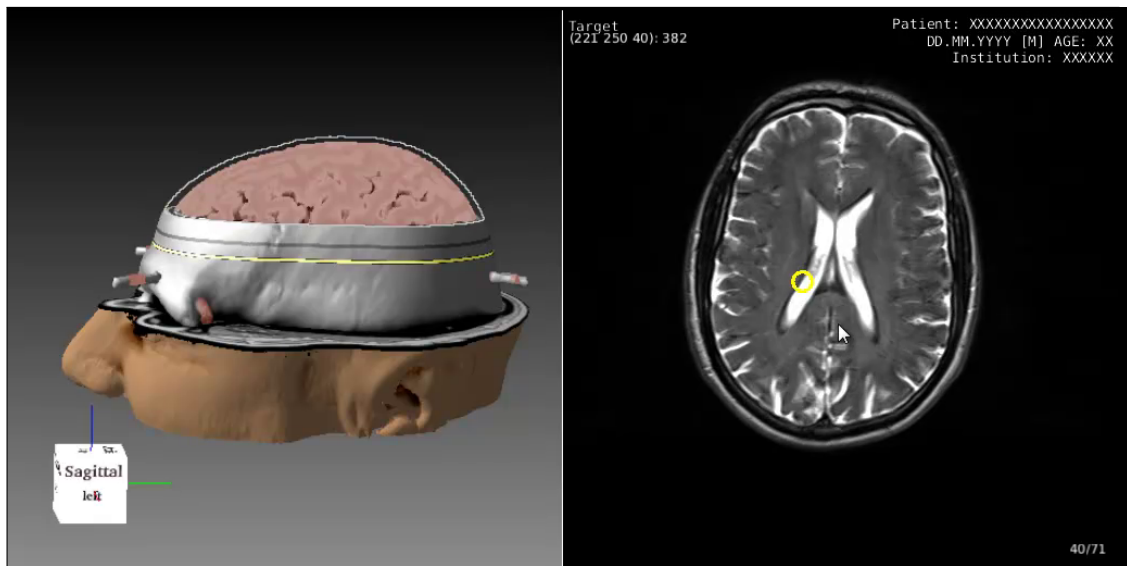


Figure 4.6: This view shows the part of the system that is used to import the results of a different planning tool to determine the entry point for the access path and the intended target location.

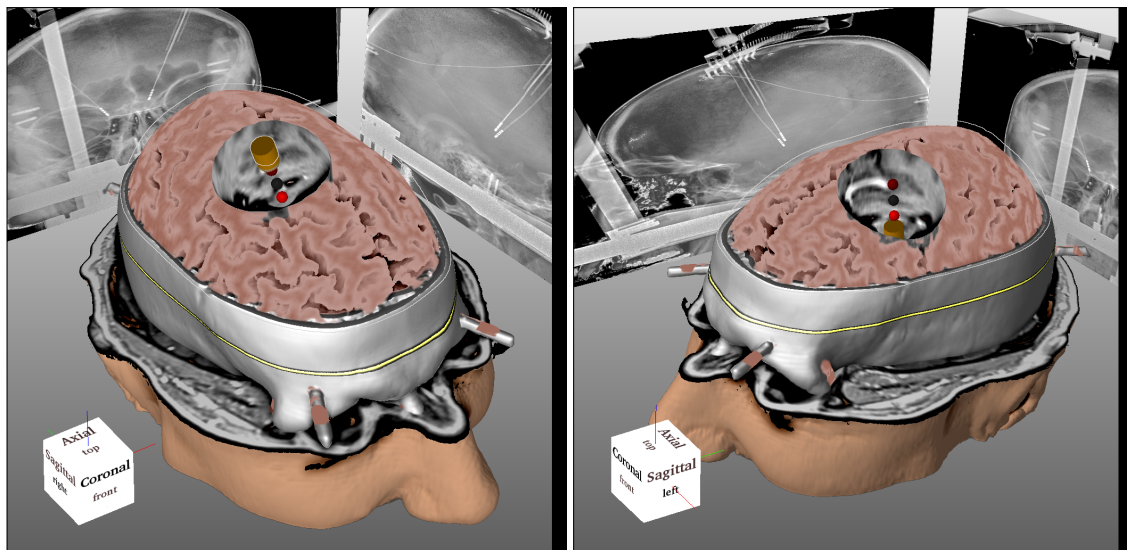
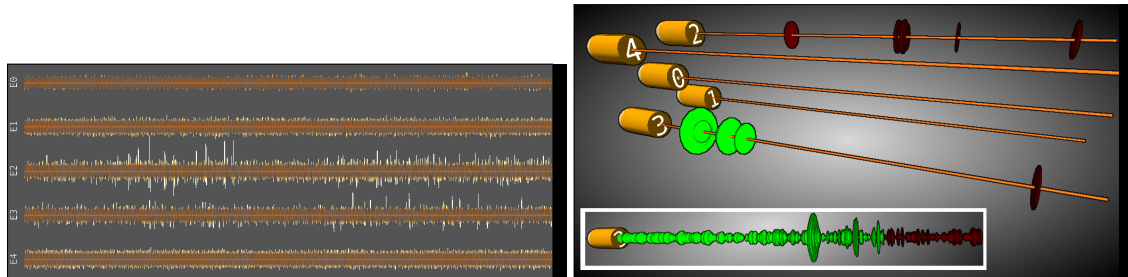


Figure 4.7: Presenting the *Contextual View* that shows the multimodal fusion of all available datasets. The preoperative CT and MRI as well as the intraoperative bi-planar X-ray scans are visible together with the animated location of the electrode. The colored beads along the access path show an automatic classification of the electrode measurements.



(a) The 2D oscilloscope rendering of the direct electrode measurements. Measurements with low amplitude are deemphasized by using darker colors.

(b) The spatial 3D rendering of the electrode rendering, showing their relative spatial location and rendering the high-amplitude measurements of the signal as colored discs.

Figure 4.8: This figure shows the two rendering methods for displaying the measurements recorded by the Microelectrode Recording electrodes. Both a view containing the accurate values are available (a) as well as a view showing the relative spatial relation between the electrodes.

802 **Contextual View** This 3D view combines the preoperational CT and MRI scans
 803 together with the bi-planar X-rays and the current electrode location (see Figure 4.7).
 804 For improve depth perception, we utilize a depth darkening effect as presented by
 805 Luft et al. [44]. The selected access path is presented in this view as a carved out
 806 tunnel along which the electrode is moved during the operation. Explicitly showing
 807 the access path serves two purposes, first, it reduces the chance of a dangerous
 808 left-right mismatch error that might otherwise occur in the operation in which the
 809 electrode is accidentally inserted into the wrong hemisphere. Second, it enables us
 810 to place colored beads inside the access path behind the electrode. The colors of
 811 these beads depend on an automatic region classification of the incoming electrode
 812 signal. This method was adopted from related works [20, 49].

813 **2D audio visualization** This view shows an augmented visualization similar to
 814 an oscilloscope that presents the direct measurements from the available electrodes.
 815 As only the amplitude and frequency are important during the procedure, we
 816 emphasize measurements that exceed a user-defined threshold and deemphasize
 817 the values below the threshold (see Figure 4.8(a)). By this technique we highlight
 818 the potentially important measurements and reducing the visual noise from the
 819 low intensity signals. This view is linked with the *3D audio visualization*, described
 820 below, such that when a specific electrode is selected in either view, it is highlighted
 821 in both views with a different color. This can be used by the surgeon to be able to
 822 correlate the detailed measurements with the relative location of the electrode.

823 **3D audio visualization** In this separate view, the relative locations of the
 824 different electrodes are displayed (see Figure 4.8(b)). The camera orientation is

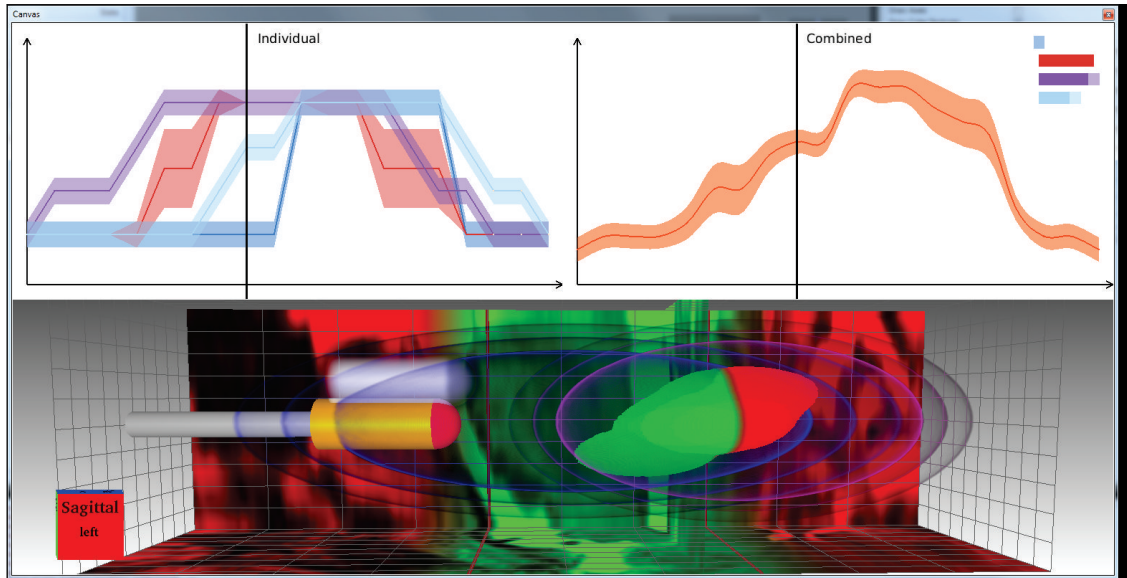


Figure 4.9: The views that show the results of the different measurements performed during the recording phase. The *Target closeup* (bottom view) contains the segmented location of the STN is visible as well as the results of the different tests at their spatial location. The *Placement guide* shows the likelihood measurements according to their depth along the access path

linked between this and the *Contextual View* such that the mental registration 825
between the two views is not broken. In this view, each electrodes' measurements 826
that exceed a user-defined threshold are shown as discs that start at the electrode 827
and move away from the electrode's base with increasing time. The size of the disc 828
corresponds to the amplitude of the detected signal and thus shows the strength 829
of the measured signal. This allows the surgeon to view the two important values 830
(amplitude and frequency) for each of the electrodes together with their spatial 831
orientation. The color of each disc is determined by the same classification algorithm 832
that is used on the beads in the *Contextual View*, but is simplified to show red if 833
the electrode is outside of the STN and green if it is inside the STN. The surgeon 834
can then, by correlating the frequency of discs and their amplitude verify that the 835
classification was correct and that the electrodes are in the correct location. 836

Target closeup After the potential electrode location has been determined, the 837
surgeon uses this closeup view, centered around the segmented location of the STN, 838
that combines all of the information that was gathered in the recording phase 839
(see Figure 4.9 bottom). Embedded in this view are the locations of the electrode 840
as determined by the depth along the access path together with their reconstructed 841
location using the biplanar X-ray scans. In addition it shows the MER signal 842
results as a red-green overlay on the backside of the bounding box and presents 843

844 options to add patient test results as additional half-transparent oval overlays. As
 845 all of these values have their own, unknown, uncertainty this view displays the
 846 overlap of the regions to inform the surgeon of a potential final placement that
 847 agrees with most measurements. On demand, the surgeon can enable the rendering
 848 of the MRI scan around the STN.

849 **Placement guide** This view is based on the same information as the *Target*
 850 *closeup*, but presents the information in a line plot, whose ordinate shows the
 851 likelihood of a correct placement for each measurement and the abscissa shows
 852 the depth along the access path (see Figure 4.9 top). We display an estimate of
 853 uncertainty for each value by extruding the line with a transparent band.

854 Evaluation

855 In order to perform an initial evaluation of the system, we conducted a qualitative
 856 user study with five neurosurgeons, which all had experience with conducting DBS
 857 interventions. Each of the participants watched the usage of the system during
 858 the planning, recording, and placement phase. The data for this test case was
 859 recorded during an operation performed by one of the coauthors. Then, each
 860 participant answered a questionnaire that used eight of the questions suggested by
 861 Martelli et al. for evaluating computer-aided surgery systems [45] with an additional
 862 free form text field for comments.

863 Generalizability

864 As mentioned in Chapter 3, one opportunity for application papers to advance the
 865 field of visualization is by providing generalizable solutions. To this end, the entire
 866 system was implemented in the Voreen framework [48], which allows the reusability
 867 of individual components. Judging the work package from this point of view, there
 868 are two parts that can provide useful in other application domains.

869 **Audio Visualization** The 3D audio visualization that is used to display the
 870 MER measurements in a spatial context can be extended to any kind of timevarying
 871 data that can be filtered by a binary filter and where the spatial location of the
 872 individual measurements is important.

873 **Uncertainty Ranges** The visualization of the uncertainty ranges in the *Target*
 874 *closeup* view might also prove beneficial to other domain areas in whcih multiple
 875 uncertain sources are used to pinpoint a most likely location of a target region.
 876 Naturally, they do not have to be isotropic uncertainties, but any form of visual
 877 feedback between spatial locations and uncertainties can be useful.

4.3 Urban Search & Rescue	878
4.4 Astrophysics	879
4.4.1 Space Weather Visualization	880
[10] [38]	881
4.4.2 Ion Beam Simulations	882
4.4.3 OpenSpace	883
[13] [11]	884
Adding CG&A in submission?	885

886

C H A P T E R

5

887

Reflections

- 888 • Getting solutions for future applications
889 • What things would make future application design easier
•

Influence on the title

Bibliography

- 891 [1] C. Abraham, P. Cornillion, E. Matzner-Løer, and N. Molinari. Unsupervised
892 curve clustering using b-splines. *Scandinavian Journal of Statistics*, 30:581–595,
893 2003. [pages [17](#) and [21](#)]
- 894 [2] Axelsson, Emil and Costa, Jonathas and Silva, Cláudio T. and Emmart, Carter
895 and Bock, Alexander and Ynnerman, Anders. Dynamic Scene Graph: Enabling
896 Scaling, Positioning, and Navigation in the Universe. In *Computer Graphics
897 Forum, Proceedings of EuroVis*, 2017 (in submission).
- 898 [3] K.-J. Bathe and E. L. Wilson. Numerical methods in finite element analysis.
899 1976. [page [15](#)]
- 900 [4] A. L. Benabid, S. Chabardes, J. Mitrofanis, and P. Pollak. Deep brain
901 stimulation of the subthalamic nucleus for the treatment of Parkinson’s disease.
902 *Lancet neurology*, 8(1):67–81, 2009. [page [22](#)]
- 903 [5] A. Benazzouz, S. Breit, A. Koudsie, P. Pollak, P. Krack, and A.-L. Benabid.
904 Intraoperative microrecordings of the subthalamic nucleus in parkinson’s
905 disease. *Movement disorders*, 17(S3):S145–S149, 2002. [page [22](#)]
- 906 [6] A. Bock, E. Sundén, B. Liu, B. Wuensche, and T. Ropinski. Coherency-Based
907 Curve Compression for High-Order Finite Element Model Visualization. *IEEE
908 TVCG (SciVis Proceedings)*, 18(12):2315–2324, 2012.
- 909 [7] A. Bock, N. Lang, G. Evangelista, R. Lehrke, and T. Ropinski. Guiding Deep
910 Brain Stimulation Interventions by Fusing Multimodal Uncertainty Regions.
911 *Proceedings of the 2013 IEEE Pacific Visualization Symposium (PacificVis)*,
912 pages 97–104, 2013.
- 913 [8] A. Bock, A. Kleiner, J. Lundberg, and T. Ropinski. Supporting Urban Search
914 & Rescue Mission Planning through Visualization-Based Analysis. In *Vision,
915 Modeling, and Visualization*, 2014.
- 916 [9] A. Bock, A. Kleiner, J. Lundberg, and T. Ropinski. An Interactive Visualiza-
917 tion System for Urban Search & Rescue Mission Planning. In *International
918 Symposium on Safety, Security, and Rescue Robotics*. IEEE, 2014.

32 Bibliography

- [10] A. Bock, M. L. Mays, L. Rastaetter, A. Ynnerman, and T. Ropinski. VCMass: 919
A Framework for Verification of Coronal Mass Ejection Ensemble Simulations. 920
Poster at IEEE VIS 2014, 2014. [page 28] 921
- [11] A. Bock, M. Marcinkowski, J. Kilby, C. Emmart, and A. Ynnerman. 922
OpenSpace: Public Dissemination of Space Mission Profiles. Poster at IEEE 923
Vis, 2015. [page 28] 924
- [12] A. Bock, A. Pembroke, M. L. Mays, L. Rastaetter, A. Ynnerman, and T. Ropin- 925
ski. Visual Verification of Space Weather Ensemble Simulations. In *Proceedings* 926
of the IEEE Vis, 2015. 927
- [13] A. Bock, A. Pembroke, M. L. Mays, and A. Ynnerman. OpenSpace: An 928
Open-Source Framework for Data Visualization and Contextualization. Poster 929
Presentation at American Geophysical Union, Fall Meeting, 2015. [page 28] 930
- [14] A. Bock, Å. Svensson, A. Kleiner, J. Lundberg, and T. Ropinski. A 931
visualization-based analysis system for urban search & rescue mission planning 932
support. In *Computer Graphics Forum*. Wiley Online Library, 2016, in press. 933
- [15] A. Bock, C. Emmart, M. Kuznetsova, and A. Ynnerman. OpenSpace: Changing 934
the narrative of public disseminations from *what to how*. In *Computer Graphics* 935
& Applications, 2017 (in submission). 936
- [16] C. R. Butson, S. E. Cooper, J. M. Henderson, and C. C. McIntyre. Patient- 937
specific analysis of the volume of tissue activated during deep brain stimulation. 938
Neuroimage, 34(2):661–670, 2007. [page 23] 939
- [17] S. K. Card, J. D. Mackinlay, and B. Shneiderman. *Readings in information* 940
visualization: using vision to think. Morgan Kaufmann, 1999. [page 5] 941
- [18] S. Carpendale. Evaluating information visualizations. In *Information Visuali-* 942
zation, pages 19–45. Springer, 2008. [page 10] 943
- [19] E. Catmull and R. Rom. A class of local interpolating splines. *Computer aided* 944
geometric design, 74:317–326, 1974. [page 16] 945
- [20] P. D’Haese, E. Cetinkaya, P. Konrad, et al. Computer-aided placement of 946
deep brain stimulators: from planning to intraoperative guidance. *IEEE* 947
Transactions on Medical Imaging, 24(11):1469–1478, 2005. [page 25] 948
- [21] M. E. Dieckmann, A. Bock, H. Ahmed, D. Doria, G. Sarri, A. Ynnerman, and 949
M. Borghesi. Shocks in unmagnetized plasma with a shear flow: Stability and 950
magnetic field generation. *Journal of Plasma Physics*, 2015. 951
- [22] R. A. Drebin, L. Carpenter, and P. Hanrahan. Volume rendering. In *ACM* 952
Siggraph Computer Graphics, volume 22, pages 65–74. ACM, 1988. [page 6] 953

- 954 [23] K. Engel, M. Hadwiger, J. Kniss, C. Rezk-Salama, and D. Weiskopf. *Real-time*
 955 *volume graphics*. CRC Press, 2006. [page 6]
- 956 [24] K. A. Ericsson and H. A. Simon. Verbal reports as data. *Psychological review*,
 957 87(3):215, 1980. [page 10]
- 958 [25] C. Everitt. Interactive order-independent transparency. *White paper, nVIDIA*,
 959 2(6):7, 2001. [page 18]
- 960 [26] C. Forsell and M. Cooper. A guide to reporting scientific evaluation in
 961 visualization. In *Proceedings of the International Working Conference on*
 962 *Advanced Visual Interfaces*, pages 608–611. ACM, 2012. [page 10]
- 963 [27] B. Guenter and R. Parent. Computing the arc length of parametric curves.
 964 *IEEE Computer Graphics & Applications*, 1990. [pages 19 and 21]
- 965 [28] M. Hadwiger, C. Sigg, H. Scharsach, K. Bühler, and M. Gross. Real-time ray-
 966 casting and advanced shading of discrete isosurfaces. In *Computer Graphics*
 967 *Forum*, volume 24, pages 303–312. Wiley Online Library, 2005. [page 6]
- 968 [29] G.-M. Hariz, M. Lindberg, and A. T. Bergenheim. Impact of thalamic deep
 969 brain stimulation on disability and health-related quality of life in patients
 970 with essential tremor. *Journal of Neurology, Neurosurgery and Psychiatry*, 72:
 971 47–52, 2002. [page 22]
- 972 [30] J. Hartigan. *Clustering Algorithms*. New York: Wiley, 1975. [pages 17 and 21]
- 973 [31] R. M. Kirby and M. Meyer. Visualization collaborations: What works and
 974 why. *IEEE computer graphics and applications*, 33(6):82–88, 2013. [pages 4
 975 and 9]
- 976 [32] R. Kosara, C. G. Healey, V. Interrante, D. H. Laidlaw, and C. Ware. Thoughts
 977 on user studies: Why, how, and when. *IEEE Computer Graphics and Applica-*
 978 *tions*, 23(4):20–25, 2003. [page 10]
- 979 [33] J. Kruger and R. Westermann. Acceleration techniques for gpu-based volume
 980 rendering. In *Proceedings of the 14th IEEE Visualization 2003 (VIS'03)*,
 981 page 38. IEEE Computer Society, 2003. [pages 6 and 18]
- 982 [34] F. Lenz, J. Dostrvsky, H. Kwan, et al. Methods for microstimulation and
 983 recording of single neurons and evoked potentials in the human central nervous
 984 system. *Journal of neurosurgery*, 68(4):630–634, 1988. [page 22]
- 985 [35] M. Levoy. Display of surfaces from volume data. *IEEE Computer graphics*
 986 *and Applications*, 8(3):29–37, 1988. [page 6]
- 987 [36] C. Lewis and J. Rieman. Task-centered user interface design. *A Practical*
 988 *Introductio*, 1993. [page 10]

34 Bibliography

- [37] R. Likert. A technique for the measurement of attitudes. *Archives of psychology*, 1932. [page 10] 989
990
- [38] S. Lindholm. *Medical Volume Visualization beyond Single Voxel Values*. PhD thesis, Linköping University, 2014. [page 28] 991
992
- [39] S. Lindholm and A. Bock. Poor Man's Rendering Of Segmented Data. In T. Ropinski and J. Unger, editors, *Proceedings of SIGRAD 2013, Visual Computing, June 13-14, 2013, Norrköping, Sweden*, volume 094, pages 49–54. Linköping University Electronic Press, 2013. 993
994
995
996
- [40] S. Lindholm, M. Falk, E. Sundén, A. Bock, A. Ynnerman, and T. Ropinski. Hybrid Data Visualization Based On Depth Complexity Histogram Analysis. *Computer Graphics Forum*, 34(1):74–85, 2014, DOI: 10.1111/cgf.12460. 997
998
999
- [41] B. Liu, A. Bock, T. Ropinski, M. Nash, P. Nielsen, and B. Wuensche. GPU-Accelerated Direct Volume Rendering of Finite Element Data Sets. In *Proceedings of the 27th Conference on Image and Vision Computing New Zealand*, pages 109–114. ACM, 2012. [page 15] 1000
1001
1002
1003
- [42] P. Ljung. Adaptive Sampling in Single Pass, GPU-based Raycasting of Multiresolution Volumes. In R. Machiraju and T. Moeller, editors, *Volume Graphics*. The Eurographics Association, 2006. [page 19] 1004
1005
1006
- [43] B. Lorensen. On the death of visualization. In *Position Papers NIH/NSF Proc. Fall 2004 Workshop Visualization Research Challenges*, volume 1, 2004. [page 5] 1007
1008
1009
- [44] T. Luft, C. Colditz, and O. Deussen. *Image enhancement by unsharp masking the depth buffer*, volume 25. ACM, 2006. [page 25] 1010
1011
- [45] S. Martelli, L. Nofrini, P. Vendruscolo, and A. Visani. Criteria of interface evaluation for computer assisted surgery systems. *International journal of medical informatics*, 72(1):35–45, 2003. [page 27] 1012
1013
1014
- [46] N. Max. Optical models for direct volume rendering. *IEEE Transactions on Visualization and Computer Graphics*, 1(2):99–108, 1995. [page 6] 1015
1016
- [47] B. H. McCormick, T. A. DeFanti, and M. D. Brown. Visualization in scientific computing, 1987. [page 4] 1017
1018
- [48] J. Meyer-Spradow, T. Ropinski, J. Mensmann, and K. Hinrichs. Voreen: A rapid-prototyping environment for ray-casting-based volume visualizations. *IEEE Computer Graphics and Applications*, 29(6):6–13, 2009. [pages 20 and 27] 1019
1020
1021
- [49] S. Miocinovic, J. Zhang, W. Xu, et al. Stereotactic neurosurgical planning, recording, and visualization for deep brain stimulation in non-human primates. *Journal of neuroscience methods*, 162(1-2):32–41, 2007. [page 25] 1022
1023
1024

- 1025 [50] T. Munzner. A nested model for visualization design and validation. *IEEE transactions on visualization and computer graphics*, 15(6):921–928, 2009.
 1026 [page 9]
- 1028 [51] T. Munzner. *Visualization Analysis and Design*. CRC Press, 2014. [page 6]
- 1029 [52] K. T. Nguyen, A. Bock, A. Ynnerman, and T. Ropinski. Deriving and
 1030 Visualizing Uncertainty in Kinetic PET Modeling. In *Proceedings of the EG*
 1031 *Visual Computing for Biology and Medicine*, pages 107–114, 2012.
- 1032 [53] J. Nielsen. Heuristic evaluation. *Usability inspection methods*, 17(1):25–62,
 1033 1994. [page 10]
- 1034 [54] C. Plaisant. The challenge of information visualization evaluation. In *Proceed-
 1035 ings of the working conference on Advanced visual interfaces*, pages 109–116.
 1036 ACM, 2004. [page 10]
- 1037 [55] B. Preim and D. Bartz. *Visualization in medicine: theory, algorithms, and
 1038 applications*. Morgan Kaufmann, 2007. [page 14]
- 1039 [56] E. Richter, T. Hogue, W. Halliday, et al. Determining the position and size
 1040 of the subthalamic nucleus based on magnetic resonance imaging results in
 1041 patients with advanced Parkinson disease. *Journal of neurosurgery*, 100(3):
 1042 541–546, 2004. [page 22]
- 1043 [57] W. W. Royce. Managing the development of large software systems. In
 1044 *proceedings of IEEE WESCON*, volume 26, pages 328–338. Los Angeles, 1970.
 1045 [page 10]
- 1046 [58] A. Rungta, B. Summa, D. Demir, P.-T. Bremer, and V. Pascucci. Manyvis:
 1047 multiple applications in an integrated visualization environment. *IEEE transac-
 1048 tions on visualization and computer graphics*, 19(12):2878–2885, 2013. [page 9]
- 1049 [59] P. Sabella. A rendering algorithm for visualizing 3d scalar fields. *ACM
 1050 SIGGRAPH computer graphics*, 22(4):51–58, 1988. [page 6]
- 1051 [60] M. Segal and K. Akeley. The opengl graphics system: A specification. Technical
 1052 report, The Khronos Group Inc, 2016. [page 5]
- 1053 [61] R. R. Shamir, I. Tamir, E. Dabool, et al. A method for planning safe trajec-
 1054 tories in image-guided keyhole neurosurgery. *MICCAI*, 13(Pt 3):457–64, 2010.
 1055 [page 23]
- 1056 [62] J. Snow. *On the mode of communication of cholera*. John Churchill, 1855.
 1057 [page 1]

36 Bibliography

- [63] P. Starr, C. Christine, P. Theodosopoulos, et al. Implantation of deep brain stimulators into the subthalamic nucleus: technical approach and magnetic resonance imaging-verified lead locations. *Journal of neurosurgery*, 97(2):1060–370–87, 2002. [page 22] 1058
1059
1060
1061
- [64] S. Stegmaier, M. Strengert, T. Klein, and T. Ertl. A simple and flexible volume rendering framework for graphics-hardware-based raycasting. In *Fourth International Workshop on Volume Graphics, 2005.*, pages 187–241. IEEE, 2005. [page 6] 1062
1063
1064
1065
- [65] E. Sundén, A. Bock, D. Jönsson, A. Ynnerman, and T. Ropinski. Interaction Techniques as a Communication Channel when Presenting 3D Visualizations. In *IEEE VIS International Workshop on 3DVis*. IEEE Digital Library, 2014. 1066
1067
1068
- [66] M. Tory and T. Möller. A model-based visualization taxonomy. *School of Computing Science, Simon Fraser University*, 2002. [page 5] 1069
1070
- [67] M. Tory and T. Moller. Human factors in visualization research. *IEEE transactions on visualization and computer graphics*, 10(1):72–84, 2004. [page 9] 1071
1072
- [68] M. Tory and T. Moller. Evaluating visualizations: do expert reviews work? *IEEE computer graphics and applications*, 25(5):8–11, 2005. [page 10] 1073
1074
- [69] E. R. Tufte. Envisioning information. *Optometry & Vision Science*, 68(4):1075
322–324, 1991. [page 3] 1076
- [70] E. R. Tufte and P. Graves-Morris. *The visual display of quantitative information*, volume 2. Graphics press Cheshire, CT, 1983. [page 3] 1077
1078
- [71] J. J. Van Wijk. The value of visualization. In *VIS 05. IEEE Visualization, 2005.*, pages 79–86. IEEE, 2005. [pages 5 and 6] 1079
1080
- [72] J. J. Van Wijk. Bridging the gaps. *IEEE Computer Graphics and Applications*, 26(6):6–9, 2006. [page 9] 1081
1082
- [73] R. Victor. Iterative and incremental development: A brief history. *IEEE Computer Society*, pages 47–56, 2003. [page 10] 1083
1084
- [74] M. Q. Wang Baldonado, A. Woodruff, and A. Kuchinsky. Guidelines for using multiple views in information visualization. In *Proceedings of the working conference on Advanced visual interfaces*, pages 110–119. ACM, 2000. [page 9] 1085
1086
1087
- [75] M. Wertheimer. Untersuchungen zur lehre von der gestalt. *Psychological Research*, 1(1):47–58, 1922. [page 3] 1088
1089

- 1090 [76] R. Westermann and T. Ertl. Efficiently using graphics hardware in volume
1091 rendering applications. In *Proceedings of the 25th annual conference on*
1092 *Computer graphics and interactive techniques*, pages 169–177. ACM, 1998.
1093 [page 6]
- 1094 [77] L. Westover. Footprint evaluation for volume rendering. *ACM Siggraph*
1095 *Computer Graphics*, 24(4):367–376, 1990. [page 6]
- 1096 [78] B. Wünsche and A. A. Young. The visualization and measurement of left ven-
1097 tricular deformation using finite element models. *Journal of Visual Languages*
1098 & Computing
- 1099 [79] A. A. Young and L. Axel. Three-dimensional motion and deformation of the
1100 heart wall: estimation with spatial modulation of magnetization—a model-based
1101 approach. *Radiology*, 185(1):241–247, 1992. [page 15]
- 1102 [80] A. A. Young, D. L. Kraitchman, L. Dougherty, and L. Axel. Tracking and
1103 finite element analysis of stripe deformation in magnetic resonance tagging.
IEEE transactions on medical imaging, 14(3):413–421, 1995. [page 15]

1105

Papers



1106

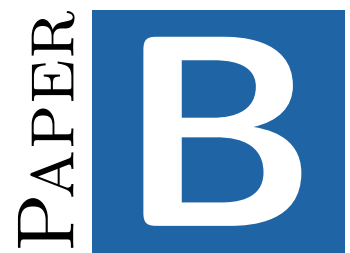
1107

Coherency-Based Curve Compression for High-Order Finite Element Model Visualization

© 2012

A. Bock, E. Sundén, B. Liu, B. Wuensche, and T. Ropinski. Coherency-Based Curve Compression for High-Order Finite Element Model Visualization. *IEEE TVCG (SciVis Proceedings)*, 18(12):2315–2324, 2012.

1108



1109

Guiding Deep Brain Stimulation Interventions by
Fusing Multimodal Uncertainty Regions

© 2013

A. Bock, N. Lang, G. Evangelista, R. Lehrke, and T. Ropinski. Guiding Deep Brain Stimulation Interventions by Fusing Multimodal Uncertainty Regions. *Proceedings of the 2013 IEEE Pacific Visualization Symposium (PacificVis)*, pages 97–104, 2013.

1110



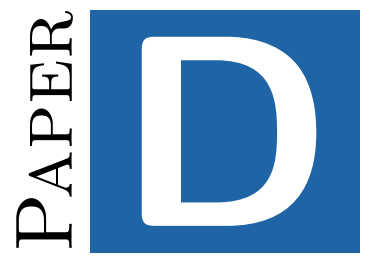
1111

Supporting Urban Search & Rescue Mission Planning
through Visualization-Based Analysis

© 2014

A. Bock, A. Kleiner, J. Lundberg, and T. Ropinski. Supporting Urban Search & Rescue Mission Planning through Visualization-Based Analysis.
In *Vision, Modeling, and Visualization*, 2014.

1112



1113

An Interactive Visualization System for Urban Search
& Rescue Mission Planning

© 2014

A. Bock, A. Kleiner, J. Lundberg, and T. Ropinski. An Interactive Visualization System for Urban Search & Rescue Mission Planning. In *International Symposium on Safety, Security, and Rescue Robotics*. IEEE, 2014.

1114



1115

A Visualization-Based Analysis System for Urban Search & Rescue Mission Planning Support

© 2016

A. Bock, Å. Svensson, A. Kleiner, J. Lundberg, and T. Ropinski. A visualization-based analysis system for urban search & rescue mission planning support. In *Computer Graphics Forum*. Wiley Online Library, 2016, in press.

1116



1117

Visual Verification of Space Weather Ensemble Simulations

© 2015

A. Bock, A. Pembroke, M. L. Mays, L. Rastaetter, A. Ynnerman, and T. Ropinski. Visual Verification of Space Weather Ensemble Simulations. In *Proceedings of the IEEE Vis*, 2015.



1118

1119

Shocks in unmagnetized plasma with a shear flow:
Stability and magnetic field generation
© 2015

M. E. Dieckmann, A. Bock, H. Ahmed, D. Doria, G. Sarri, A. Ynnerman,
and M. Borghesi. Shocks in unmagnetized plasma with a shear flow:
Stability and magnetic field generation. *Journal of Plasma Physics*, 2015.

1120



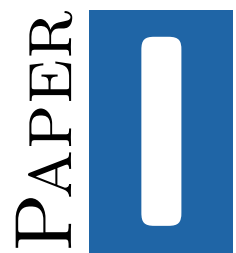
1121

Hybrid Data Visualization Based On Depth Complexity Histogram Analysis

© 2014

S. Lindholm, M. Falk, E. Sundén, A. Bock, A. Ynnerman, and T. Ropinski.
Hybrid Data Visualization Based On Depth Complexity Histogram Analysis.
Computer Graphics Forum, 34(1):74–85, 2014, DOI: 10.1111/cgf.12460.

1122



1123

Dynamic Scene Graph: Enabling Scaling, Positioning, and Navigation in the Universe

© 2017

Axelsson, Emil and Costa, Jonathas and Silva, Cláudio T. and Emmart, Carter and Bock, Alexander and Ynnerman, Anders. Dynamic Scene Graph: Enabling Scaling, Positioning, and Navigation in the Universe. In *Computer Graphics Forum, Proceedings of EuroVis*, 2017 (in submission).

1124

1125

OpenSpace: Changing the narrative of public
disseminations from *what* to *how*

© 2017

A. Bock, C. Emmart, M. Kuznetsova, and A. Ynnerman. OpenSpace:
Changing the narrative of public disseminations from *what* to *how*. In
Computer Graphics & Applications, 2017 (in submission).

